

An Islanded Microgrid Droop Control using Henry Gas Solubility Optimization



Mohamed A. Ebrahim, Reham M. Abdel Fattah, Ebtisam M. Saied, Samir M. Abdel Maksoud, Hisham El Khashab

Abstract: Coordination of various distributed generation (DG) units is required to meet the growing demand for electricity. Several control strategies have been developed to operate parallel-connected inverters for microgrid load sharing. Among these techniques, due to the lack of essential communication links between parallel-connected inverters to coordinate the DG units within a microgrid, the droop control method has been generally accepted in the scientific community. This paper discusses the microgrid droop controller during islanding using the Henry Gas Solubility Optimization (HGSO). The most important goals of droop control in the islanded mode of operation are the frequency and voltage control of microgrid and proper power sharing between distributed generations. The droop controller has been designed using HGSO to optimally choose PI gains and droop control coefficients in order to obtain a better microgrid output response during islanding. Simulation results indicate that the droop controller using HGSO improves the efficiency of micro-grid power by ensuring that variance in microgrid frequency and voltage regulation and effective power sharing occurs whenever micro-grid island mode or when variation in load occurs.

Keywords: Distributed generator; Droop control; Henry Gas Solubility Optimization; Microgrid

I. INTRODUCTION

The interdependence of small-generation systems such as solar photovoltaics, micro turbines, fuel cells, wind turbines and energy storage devices to the low-voltage distribution network will contribute to a dynamic power grid. Such power sources have decentralized generation capabilities and are known as distributed generators (DGs) [1]. A microgrid consists of local loads and sources of distributed generation (DGs).

Revised Manuscript Received on January 08, 2021.

* Correspondence Author

Mohamed A. Ebrahim*, Electrical Engineering Department, Faculty of Engineering at Shoubra, Benha University, Cairo, Egypt. Email: Mohamed.mohamed@feng.bu.edu.eg

Reham M. Abdel Fattah, Power Electronics and Energy Conversion Department, Electronics Research Institute, Cairo Egypt. Email: reham@eri.sci.eg

Ebtisam M. Saied, Electrical Engineering Department, Faculty of Engineering at Shoubra, Benha University, Cairo, Egypt and Electrical Engineering Department-High Technological Institute (HTI)10th of Ramadan City-Egypt. Email: Ebtisam.saied@feng.bu.edu.eg

Samir M. Abdel Maksoud, Electrical Engineering Department, Faculty of Engineering at Shoubra, Benha University, Cairo, Egypt. Email: Samir.abdelmaksoud@feng.bu.edu.eg

Hisham El Khashab, Power Electronics and Energy Conversion Department, Electronics Research Institute, Cairo Egypt. Email: khashab@eri.sci.eg

© The Authors. Published by Blue Eyes Intelligence Engineering and Sciences Publication (BEIESP). This is an open access article under the CC BY-NC-ND license (<http://creativecommons.org/licenses/by-nc-nd/4.0/>)

A microgrid can operate in two different modes of operation. Microgrid must work both in the grid-connected mode and in the island contingency mode. In grid-connected mode, it is linked to the main grid, being delivered from or injecting power into it. The island operation mode is another mode and the microgrid is separated from the distribution network [2]. DGs increase service efficiency and reduce the need to prepare for future generation expansion. The proper control target for DGs in a microgrid is to obtain optimal power sharing while monitoring the voltage magnitude and frequency of the microgrid. There are two types of controls: the centralized Microgrid Control and the decentralized Microgrid Control. The centralized control of a microgrid that depends on a communication infrastructure. Nevertheless, inefficient and expensive to use communication links in remote areas with long distances between inverters [3]. Decentralized controllers are studied to remove communication links. By means of droop controllers, power sharing for microgrid generators is thus achieved [4]. Although the overall power quality factors can be improved by these control methods, they have difficulties in changing control parameters. In order to fulfill the power quality requirements and to ensure effective operation of the MG system, a reliable control strategy is ultimately required for both the grid-connected and island-connected modes of operation. It is important to note that the absence of inertia and ambiguity in the choosing of optimal gains of the controller Proportional Integral (PI) causes large differences in the islanded mode's power, voltage and frequency level compared to the grid-connected mode of MG operation. Therefore, this research is performed to answer these concerns and improve the efficiency of MG in the island mode of operation. With the growth of different optimization algorithms to solve several algorithms and engineering issues, the question is still open, "is there only optimization technique capable of solving all problems?" [2]. Several optimization algorithms have recently appeared, such as salp swarm inspired algorithm (SSIA) [5], moth-flame optimization techniques [6], sine cosine algorithm (SCA) [7], ant lion optimizer (ALO) [8], grey wolf optimizer (GWO) [9] and dragonfly algorithm (DA) [10] have been used with adequate convergence efficiency to achieve the optimal solution. The study suggests a Henry Gas Solubility Optimization (HGSO) based controller to optimize the PI controller parameters and droop control coefficients to obtain the optimum system behavior of an island microgrid. The HGSO is one of the most recent algorithms for optimization implemented [11]. This study uses HGSO to solve the issue finding the optimal PI parameters and droop control coefficients under the conditions of load change to regulate voltage,



frequency and power sharing of an islanded MG. In order to verify the efficacy of the proposed method, the HGSO-based droop controller performance is compared with that of the PSO and ALO-based controllers for the same.

II. HGSO HISTORY

In 2019, a new mathematical model called HGSO, which depends on Henry's Law simulations to solve optimization problems, was proposed by Fatma et al. William Henry proposed Henry's bill, a law on Henry, in 1803. The Law of Henry states that "At a constant temperature, the amount of a given gas that dissolves in a given type and volume of liquid is directly proportional to the partial pressure of that gas in equilibrium with that liquid". Consequently, Henry's law is heavily dependent on temperature [12] and shows that the solubility of gas (S_g) is proportional to the partial gas pressure (P_g), H is Henry's constant, as indicated in the following equation, which is special to the combination of gases and solvents at the temperature given:

$$S_g = H \times P_g \quad (1)$$

A. Mathematical model from HGSO

This part addresses the HGSO algorithm's mathematical equations. As follows, the HGSO mathematical model includes of eight phases [11]:

phase 1: Initialization process.

The number of gases (population size N) and gas positions are initialized calculated using the following formula:

$$Z_i(t+1) = Z_{\min} + r \times (Z_{\max} - Z_{\min}) \quad (2)$$

Where

Z_i : the position of the i^{th} gas in population N.

r : the random number between 0 and 1.

Z_{\max} , Z_{\min} : the limits of the problem

t : the time of Iteration.

i : the gas number.

$H_j(t)$: Henry's coefficient for cluster j

$P_{i,j}$: Partial gas pressure I in cluster J.

$$H_i(t) = a_1 \times \text{rand}(0,1)$$

$$P_{i,j} = a_2 \times \text{rand}(0,1)$$

$$C_j = a_3 \times \text{rand}(0,1)$$

Where, parameters are $\alpha_1, \alpha_2, \alpha_3$ with values equal to (5E-02, 100 and 1E-02).

phase 2: Clustering.

According to the number of gas groups, the agents of the population are grouped into equivalent clusters. Each cluster has identical gases and therefore has the similar constant value of Henry (H_j).

phase 3: Evaluation.

Cluster j is evaluated to determine the best gas in its shape, which is the highest equilibrium level of the others. Consequently, on the basis of having the best gas in the swarm, the gases are chosen.

phase 4: Henry Coefficient Update

The Henry coefficient is updated in accordance with the following equation:

$$H_j(t+1) = H_j(t) \times \exp(-C_j \times (\frac{1}{T(t)} - \frac{1}{T^0})) \quad (3)$$

$$T(t) = \exp(-\frac{t}{\text{iter}}) \quad (4)$$

Where

T: the temperature.

T^0 : a constant and equal to 298.15.

iter: the total number of iterations.

phase 5: Update solubility.

Solubility is updated in accordance with the following equation:

$$S_{i,j}(t) = K \times H_i(t+1) \times P_{i,j}(t) \quad (5)$$

where

$S_{i,j}$: solubility in cluster j of gas i

$P_{i,j}$: the partial gas pressure i in cluster j.

K: a constant.

phase 6: Update position.

The position will be modified with the following equation:

$$Z(t+1) = Z_{i,j} + F \times r \times \gamma \times (Z_{i,best}(t) - Z_{i,j}(t)) + F \times r \times \alpha \times (S_{i,j}(t) \times Z_{best}(t) - Z_{i,j}(t)) \quad (6)$$

$$\gamma = \beta \times \exp(-\frac{F_{best}(t) + \epsilon}{F_{i,j}(t) + \epsilon}) \quad \epsilon = 0.05 \quad (7)$$

Where

$Z_{i,j}$: gas i position in cluster j.

r : a random constant.

t : the iteration time.

$Z_{i,best}$: in cluster j, the best gas i.

Z_{best} : the best gas out of the swarm.

γ : the capability of gas j in cluster i to relate with the gases in its cluster.

a : the effect of other gases on gas i in cluster j and equal to 1

β : a constant.

$F_{(i,j)}$: the fitness of gas i in cluster j.

F_{best} : the fitness of the best gas in the entire system.

F: The flag that changes the search agent direction and gives the diversity = \pm .

$Z_{(i,best)}$ and Z_{best} are the two parameters accountable for matching the capabilities of exploration and extraction.

phase 7: Escape from local optimum.

This process is used to prevent optimal local ones. Rank and pick the worst number of agents (N_w) by using the equation below:

$$N_w = N \times (\text{rand}(C_1 - C_2) + C_1), \quad C_1 = 0.1 \text{ and } C_2 = 0.2 \quad (8)$$

Where

N : number of agents for the search.

phase 8: Position improve for the worst agents.

$$G_{(i,j)} = G_{\min(i,j)} + r \times (G_{\max(i,j)} - G_{\min(i,j)}) \quad (9)$$

Where

$G_{(i,j)}$: in cluster j , the position of gas i .

r : random number.

G_{\min} , G_{\max} : the bounds of the problem.

HGSO has many benefits, such as the search agents are split into groups and each group has the same gas coefficient, the position change referring to the solubility value of the objective function using Eq. (6). In general, since it decreases the number of operators to be tuned into HGSO, the algorithm is simple to implement and understand.

III. THE MICROGRID DROOP CONTROL TECHNIQUE

The Turbine Governor (TG) and the Automatic Voltage Regulator (AVR) are used in a traditional power system to keep both the voltage and the frequency within bounds. Regrettably, in PVS and FC systems, TG and AVR cannot be used because they are not acceptable for these systems. One of the research tasks is to find an effective solution for preserving voltage and frequency by droop control during any load increase for these purposes. Droop control is a generator control technique typically used to enable parallel generator operation and is a sample control used in the microgrid. The coupling between active power and frequency, as well as reactive power and voltage is the basic rule upon which to depend droop control. The droop control has advantages of locally measured data, does not need communication signal, high reliability, simple structure, easy implementation, and different power ratings [13]. Fig. 1 illustrates the microgrid control strategy topology, consisting of three layers of power calculation, voltage controller and current.

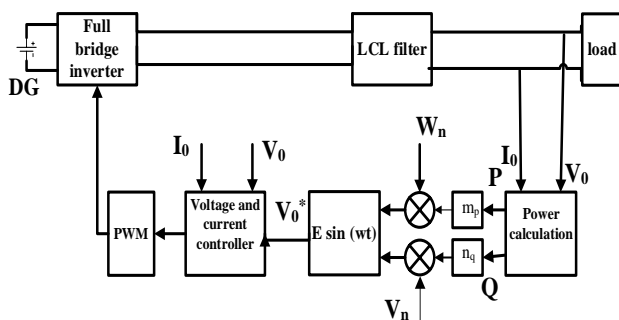


Fig.1 shown the block diagram of the system

A) Power Control

Four components are used in the power circuit: the three-phase VSI, the resistive-inductive-capacitive (RLC) filter, the coupling inductor (L_2), and the three-phase load.

B) Droop Control

Droop control is a method of control usually used for generators to enable the microgrid to operate parallel generators. The relation between the active power and the frequency and the reactive power and the voltage is centered on [13]. Using the output voltage (V_0) and output current (I_0) to determine the active power (p) and the reactive power (q) before the filter, V_0 and I_0 are translated to the dq reference frame for the calculation of (p) and (q) using the equations below:

$$p = V_{od} I_{od} + V_{oq} I_{oq} \quad (10)$$

$$q = V_{od} I_{oq} - V_{oq} I_{od} \quad (11)$$

P and Q are the result of passing p and q in the low pass filter to improve them. P and Q are computed in accordance with the equations below, respectively:

$$P = \frac{\omega_c}{S + \omega_c} (V_{od} I_{od} + V_{oq} I_{oq}) \quad (12)$$

$$Q = \frac{\omega_c}{S + \omega_c} (V_{od} I_{oq} - V_{oq} I_{od}) \quad (13)$$

The reference angular frequency ω and the reference voltage V will be determined by the equations below after the P and Q calculations:

$$\omega = \omega_n - m_p \times P \quad (14)$$

$$V = V_n - n_q \times Q \quad (15)$$

Where ω_n and V_n are the constant coefficients of frequency and voltage characteristics, respectively and m_p , n_q are the coefficients of static droop.

C) Voltage-Current Controller

An input to the voltage controller to determine the reference current (I_i^*) would be the reference voltage and frequency. I_i^* output of the voltage controller will be passed into the current controller. The output of the current controller (V^*) feeds the pulse width modulation (PWM). To control VSI, the output of PWM is used. The equations below are employed to determine I_i^* and V^* [14] :

$$I_i^* = -\omega C_f V_o^* + k_{pv} (V_o^* - V_o) + \frac{k_{iv}}{s} (V_o^* - V_o) \quad (16)$$

$$V^* = -\omega L_f I_i^* + k_{pc} (I_i^* - I_i) + \frac{k_{ic}}{s} (I_i^* - I_i) \quad (17)$$

Where

L_f : inductor of coupling

ω : frequency cut-off

S : Laplace transform parameter

Through the use of the PI controller, voltage and current are regulated.

The PI controller's gains must be measured accurately. To calculate PI gains, many methods are used, such as the trial-and-error method and root locus. These technologies are incapable of controlling complex nonlinear systems, such as microgrid systems, or even determining the accurate gains of controllers. The computation of PI gains is therefore very important, so this paper will attempt to find the PI controller's optimal gains by using the HGSO.

IV. USAGE OF HGSO IN MICROGRIDS

To determine the optimal control parameters and droop control coefficients when there is a load variation, the HGSO technique will be used. Control parameters and droop coefficients (K_{p1} , K_{i1} , K_{p2} , K_{i2} , K_{p3} , K_{i3} , K_{p4} , K_{i4} , n_q , m_p) are produced by HGSO for the realization of minimized voltage and frequency variability. In order to perform their assigned task, every optimization technique requires an objective function. For minimize the error between the voltage calculated and expected, the objective function is used. The four types of objective functions of the error benchmark are integral of absolute error (IAE), integral of square error (ISE), integral of time absolute error (ITAE), integral of time square error (ITSE) [15]. ITAE is the most commonly used feature for minimizing control goals in researchs. That's because, compared to its rivals, ITAE enables for easier implementation and provides improved results. The ITSE and ISE are aggressively criteria and, due to squaring of the error made, generate unrealistic evaluation. In contrast to the ITAE, the IAE is also an ineffective choice, reflecting reasonable a more practical error index due to the time-multiplying error feature. Equation below describes ITAE mathematically:

$$ITAE = \int_0^{\infty} t \cdot |e(t)| dt \quad (18)$$

The multi-objective function is used to recognize both the frequency and voltage errors via the accumulative sum property during this study. Fig.2 Introduces a schematic of the system of testing consisting of two solar PV array (SPVAS) systems, a DC-DC boost converter, two battery stations (BSs), a supercapacitor (SC), a three-phase VSI, a load, and a transmission line is presented. Supercapacitors are also used to increase the dynamic response of the microgrid due to their fast charging and discharging characteristics. DC-DC boost converter has a maximum power point monitoring (MPPT) dependent on incremental conductance (INC) to control the DC voltage of the SPVAS output terminals. The variables of the test system are listed in Table 1. [16]. For three optimization techniques, the detailed comparative analysis is given in Table 2. The analysis indicates that HGSO performed the given control task successfully with minimal voltage and frequency errors. For fair comparison, three alternative optimization methods (HGSO, PSO and ALO) are used to validate SSIA quality.

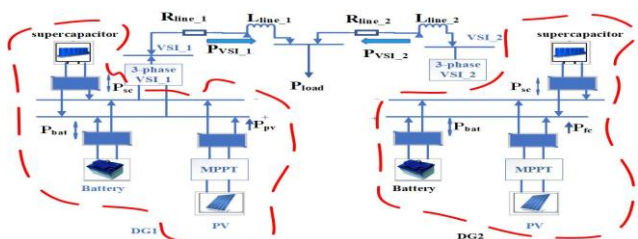


Fig.2. test system diagram

TABLE 1. variables of test system [16]

variables	Value	variables	Value
V_{base}	380 V	ω_n	1 p.u.
S_{base}	100 kVA	V_n	1 p.u.
ω_{base}	314 rad/sec	R_{line1}	0.14 p.u.
L_f	0.95×10^{-3} p.u.	L_{line1}	2.1×10^{-3} p.u.
C_f	35×10^{-6} p.u.	R_{line2}	0.2 p.u.
R_f	0.067 p.u.	L_{line2}	3.5×10^{-3} p.u.
L_c	0.23×10^{-3} p.u.	P_{load}	70×10^3
R_c	0.02 p.u.	ω_c	0.1 p.u.
T_s	5.144×10^{-6} sec	Frequency of PWM	10 kHz
Power of PV	109.88 kW	Capacitance of supercapacitor	29 F
Power of battery	56kW		

TABLE 2. Results of the three Optimization Techniques applied

	PSO	ALO	HGSO
Objective function	12.66×10^6	11.22×10^6	5.8613×10^6
K_{p1}	0.557908	0.532215	0.45173
K_{i1}	475.0824	521.9489	257.9713
K_{p2}	0.513765	0.537495	0.468047
K_{i2}	565.1678	537.8442	387.772
K_{p3}	13.09909	14.58615	13.99621
K_{i3}	12410.52	6500.108	10480.54
K_{p4}	13.05646	7.378885	5.413205
K_{i4}	11132.63	10557.64	11112.94
n_q	0.225909	0.367958	0.315453
m_p	0.009724	0.014005	0.010452
Time Taken (min)	219.1358	212.2842	296.0268

V. RESULTS IN SIMULATION

Perhaps the best controllers via HGSO are equipped with a microgrid test system to validate the power sharing between various sources as well as voltage and frequency control. In this analysis, the two types of loads are regarded with RERs variability, such as continuous change and ramp loads with the change in temperature and irradiance

Case I: Fixed Cyclic Load in Islanding Mode (FCLIM)

For islanded MG with a 70 kW (0.7p.u.) constant load, RERs variability (variable solar irradiance and temperature) is taken into account in this case. Fig.3 illustrates the rise-up / down solar irradiance from 1000 W/m² to 250 W/m². Fig.4 establishes the temperature difference between 25 °C and 50 °C. For each source, the dynamic active power response is presented in Fig.5. It should be noted that for both sources, the active power is almost equal (0.35 p.u.), which confirms successful power sharing. Remarkably, it is observed that solar radiation and temperature fluctuations do not impact power sharing because the total power fed to the DC bus is constant due to the mechanism of energy management. Fig.6 and Fig.7 During the applied case, the frequency and voltage responses are indicated. Fig.8 shows the process of energy management among the multi-sources of MG (SPVAS, BS, and SC). Throughout that interval, SC discharges, owing to the fast response of SC, to compensate for the amount of power lost until the battery takes an act to provide the load with the necessary power.



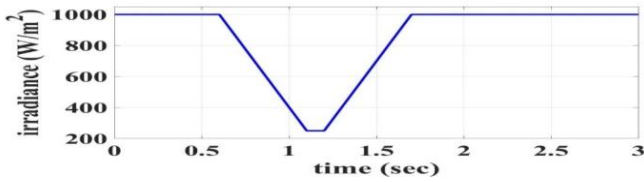


Fig. 3 Pattern of solar irradiance variance for all scenarios

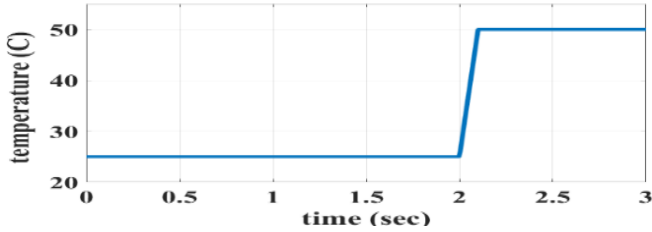


Fig. 4. Solar temperature variance for all scenarios

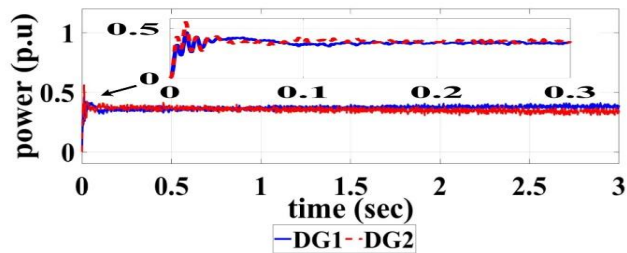


Fig.5 Active powers produced by two DGs in FCLIM scenario

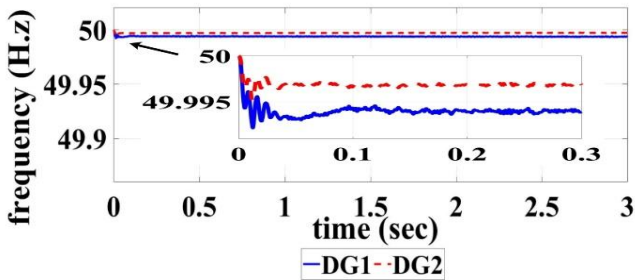


Fig.6 Inverter frequency in FCLIM scenario

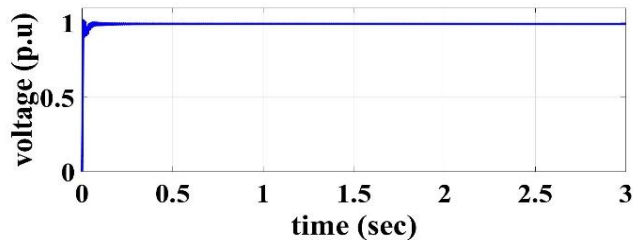


Fig.7 Voltage magnitude in FCLIM scenario

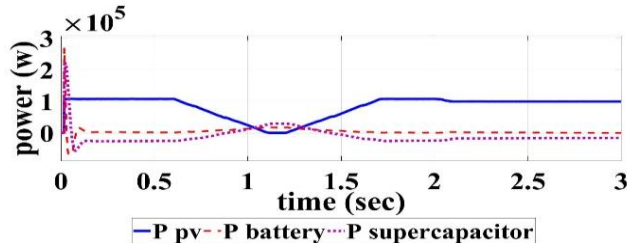


Fig.8 SPVAsSs, BSs, and SC powers in FCLIM

A. Case III: Continuous Cyclic Load in Islanding Mode Scenario (CCLIM)

- Through RERs variability, the microgrid is operated in islanding mode with continuous cyclic load variations as 70 kW (0.7 p.u.) from 0- 0.7 sec, then the load value increased to 110 kW (1.1 p.u.) at 0.7- 1.5 sec, then the load value returned to 70 kW (0.7 p.u.) at 1.5-2.5 sec at the end

of the load period. Fig.9 illustrates that an equivalent amount of active power is inserted into microgrid by each DG. In particular, the rate of power change is almost the similar as the load change rate, which supports the efficient droop control monitoring behavior based on HGSO during the CCLIM case. Fig.10 and Fig.11 During the CCLIM case, reflects the transient response of voltage and frequency. Additionally, Fig.12 illustrates, dynamic way, in which the SPVAsSs, BSs, and SC collaborate with each other to maintain supply consistency.

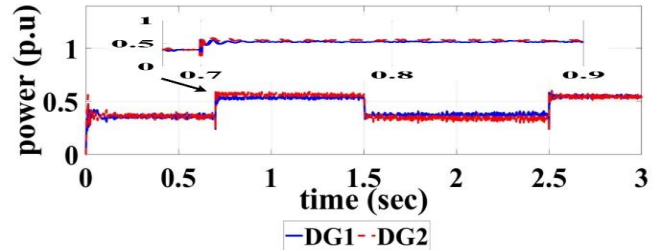


Fig.9 Active powers produced by two DGs in CCLIM scenario

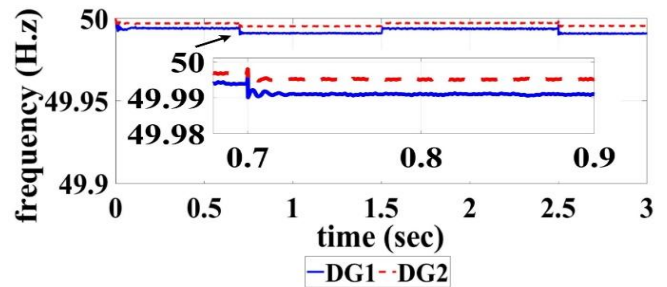


Fig.10 Frequency in inverter in CCLIM scenario

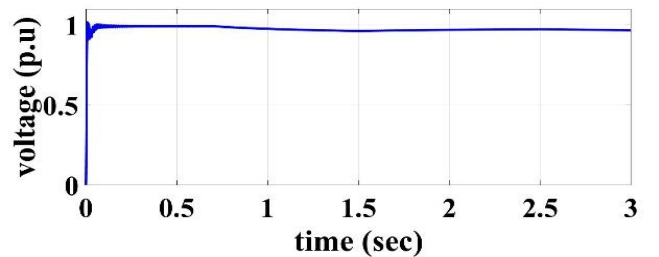


Fig.11 Magnitude of voltage in CCLIM scenario

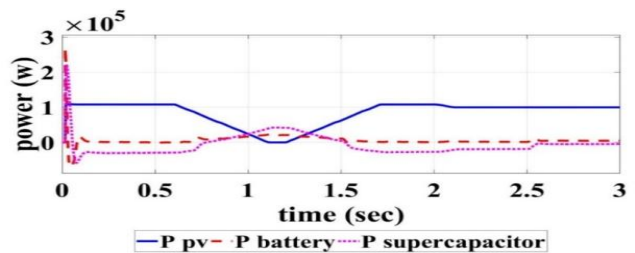


Fig.12 SPVAsSs, BSs, and SC powers in CCLIM scenario

VI. CONCLUSION

In this paper, an optimal voltage and frequency control and power sharing system for inverter-dependent DG units in an islanded microgrid was proposed based on HGSO. There are two sources and each source of a microgrid test system. It includes solar PV array, supercapacitor and battery station.

The HGSO is used to calculate the gains of the PI controllers and the droop control system coefficients. Four forms are included in the cost function: IAE, ISE, ITAE, and ITSE. Although ITAE is implemented as an objective function, the best solution is achieved. In two scenarios, the achieved gains of PI controllers and droop control coefficients K_{p1} , K_{i1} , K_{p2} , K_{i2} , K_{p3} , K_{i3} , K_{p4} , K_{i4} , n_q , m_p are implemented in the system. Fixed load and slow and rapid changes are considered in the suggested scenarios, as well as abrupt changes in both renewable energy supplies and loads. The simulated results showed that the power sharing between the parallel DGs and the droop control strategy dependent on HGSO. The frequency deviation is within the permissible range and changes in load with a good dynamic response are easily followed by the DGs had been achieved.

REFERENCES

1. Khaledian, Amir, and Masoud Aliakbar Golkar. "Analysis of droop control method in an autonomous microgrid." *Journal of applied research and technology* 15.4 (2017): 371-377.
2. M. A. Ebrahim, R. M. A. Fattah, E. M. Saied, S. M. A. Maksoud, and H. El Khashab, "Real-Time Implementation of Self-Adaptive Salp Swarm Optimization-based Microgrid Droop Control," *IEEE Access*, vol. 8, pp. 1–1, 2020, doi: 1109/access.2020.3030160.
3. T. L. Vandoor, J. M. Guerrero, D. M. de Koning, J. C. Vasquez, and L. Vandevelde, "Decentralized and centralized control of islanded microgrids including reserve management," *IEEE Ind. Electron. Mag.*, pp. 1–14, 2013.
4. Y. W. Li and C. N. Kao, "An accurate power control strategy for power-electronics-interfaced distributed generation units operating in a low-voltage multibus microgrid," *IEEE Trans. Power Electron.*, vol. 24, no. 12, pp. 2977–2988, 2009, doi: 0.1109/TPEL.2009.2022828.
5. S. Mirjalili, A. H. Gandomi, S. Z. Mirjalili, S. Saremi, H. Faris, and S. M. Mirjalili, "Salp Swarm Algorithm: A bio-inspired optimizer for engineering design problems," *Adv. Eng. Softw.*, vol. 114, pp. 163–191, 2017, doi: 10.1016/j.advengsoft.2017.07.002.
6. N. Aouchiche, M. S. Aitcheikh, M. Becherif, and M. A. Ebrahim, "AI-based global MPPT for partial shaded grid connected PV plant via MFO approach," *Sol. Energy*, vol. 171, no. August, pp. 593–603, 2018, doi: 10.1016/j.solener.2018.06.109.
7. K. Dasgupta, P. Kumar, and V. Mukherjee, "Power flow based hydro-thermal-wind scheduling of hybrid power system using sine cosine algorithm," *Electr. Power Syst. Res.*, vol. 178, no. September 2019, p. 106018, 2020, doi: 10.1016/j.epr.2019.106018.
8. M. Maher, M. A. Ebrahim, E. A. Mohamed, and A. Mohamed, "Ant-lion inspired algorithm based optimal design of electric distribution networks," *2017 19th Int. Middle-East Power Syst. Conf. MEPCON 2017 - Proc.*, vol. 2018-Febru, no. December, pp. 613–618, 2018, doi: 10.1109/MEPCON.2017.8301244.
9. S. Mirjalili, S. M. Mirjalili, and A. Lewis, "Grey Wolf Optimizer," *Adv. Eng. Softw.*, vol. 69, pp. 46–61, 2014, doi: 10.1016/j.advengsoft.2013.12.007.
10. L. Li, X. Zhao, M. Tseng, and R. R. Tan, "Short-term wind power forecasting based on support vector machine with improved dragon fly algorithm," *J. Clean. Prod.*, vol. 242, p. 118447, 2020, doi: 10.1016/j.jclepro.2019.118447.
11. F. A. Hashim, E. H. Houssein, M. S. Mabrouk, and W. Al-atabany, "Henry gas solubility optimization : A novel physics-based algorithm," *Futur. Gener. Comput. Syst.*, vol. 101, pp. 646–667, 2019, doi: 10.1016/j.future.2019.07.015.
12. Li, Yuhong, et al. "Henry's law and accumulation of weak source for crust-derived helium: A case study of Weihe Basin, China." *Journal of Natural Gas Geoscience* 2.5-6 (2017): 333-339.
13. A. Khaledian, A. Ahmadian, and M. Aliakbar-Golkar, "Optimal droop gains assignment for real-time energy management in an islanding microgrid: A two-layer techno-economic approach," *IET Gener. Transm. Distrib.*, vol. 11, no. 9, pp. 2292–2304, 2017, doi: 10.1049/iet-gtd.2016.1718.
14. K. Yu, Q. Ai, S. Wang, J. Ni, and T. Lv, "Analysis and Optimization of Droop Controller for Microgrid System Based on Small-Signal Dynamic Model," *IEEE Trans. Smart Grid*, vol. 7, no. 2, pp. 695–705, 2016, doi: 10.1109/TSG.2015.2501316.
15. K. M. Hussain, R. A. R. Zepherin, M. S. Kumar, and S. M. G. Kumar,

- "Comparison of PID Controller Tuning Methods with Genetic Algorithm for FOPTD System," *J. Eng. Res. Appl.*, vol. 4, no. 2, pp. 308–314, 2014.
16. M. Kohansal, G. B. Gharehpetian, and M. Abedi, "An optimization to improve voltage response of VSI in islanded Microgrid considering reactive power sharing," *2012 2nd Iran. Conf. Renew. Energy Distrib. Gener. ICREDG 2012*, pp. 127–131, 2012, doi: 10.1109/ICREDG.2012.6190447.

AUTHORS PROFILE



Mohamed Ahmed Ebrahim Mohamed received his B.Sc., M.Sc. and Ph.D. degrees in electrical engineering from Faculty of Engineering at Shoubra, Benha University, Cairo, Egypt, in 2004, 2009 and 2013 respectively. Mohamed took up the rank of Demonstrator, Assistant Lecturer and a Lecturer in Benha University in 2005, 2009 and 2013, respectively and associate professor since 2018. His research interests include analysis, design, and control of electric power systems, new and renewable energy applications. He published 63 scientific papers and 5 book chapters in international book series. He did several post-doctoral research missions with the Federation of Research of Fuel Cells and the University of Technology of Belfort-Montbéliard, Belfort, France. He is the PI and coordinator of different Egyptian-French projects. He is a reviewer for several IEEE Transactions, IET and different Elsevier journals.



Reham Mohamed Abd El Fattah received her B.Sc. and M.Sc. degrees in electrical engineering from Faculty of Helwan University, Cairo, Egypt, in 2004 and 2011, respectively. Her research interests included renewable energy, microgrid and optimization technique



Ebtisam Mostafa Mohamed Saied received her B.Sc., M.Sc. and Ph.D. degrees in electrical engineering from Faculty of Engineering Cairo University, Cairo, Egypt, in 1982, 1986 and 1992 respectively. Since 2003, she became a Professor of electrical engineering from Faculty of Engineering at Shoubra, Benha University, Cairo, Egypt. Her research interests include Electrical Power Engineering, power system and renewable energy applications.



Samir Mohamed Abd El Maksoud received his B.Sc., M.Sc. and Ph.D. degrees in electrical engineering from Faculty of Engineering at Shoubra, Zagazig University (Benha Branch), Cairo, Egypt, in 1983, 1992 and 2003 respectively. His research interests include analysis, Electrical Power Engineering, power system and Economic Load Dispatching Voltage instability



Hisham El Khashab was born in Cairo, Egypt, in 1952. He obtained his B.Sc and M. Sc. in 1973 and 1977, respectively, from Cairo University, Egypt. He received the Ph. D degree in electrical engineering from the National Institute of Polytechnics of Grenoble, France, in May 1982. Since 1996, he became a Professor of the power electronics and energy conversion department of Electronics Research Institute, National Research Centre of Cairo. His current research interests include power electronics, electrical machines and drives, and renewable energy. He supervised several M.Sc. and Ph.D. Theses. In 2004, he was a visiting professor at Yanbu Industrial College for ten years. He participated in establishing a renewable energy center for education and society awareness. His main research areas of interest are renewable energy systems, micro-grid control, and power electronics.

